New Probe of Departures from General Relativity Using Minkowski Functionals

Wenjuan Fang,[1,2,*] Baojiu Li,[3,†] and Gong-Bo Zhao[4,5,‡]

[1]*Department of Astronomy, University of Science and Technology of China, Hefei, Anhui 230026, People's Republic of China*
[2]*Key Laboratory for Research in Galaxies and Cosmology, Chinese Academy of Sciences,*
Hefei, Anhui 230026, People's Republic of China
[3]*Institute for Computational Cosmology, Department of Physics, Durham University, Durham DH1 3LE, United Kingdom*
[4]*National Astronomy Observatories, Chinese Academy of Science, Beijing 100012, People's Republic of China*
[5]*Institute of Cosmology and Gravitation, University of Portsmouth, Portsmouth PO1 3FX, United Kingdom*
(Received 26 January 2017; published 2 May 2017)

The morphological properties of the large scale structure of the Universe can be fully described by four Minkowski functionals (MFs), which provide important complementary information to other statistical observables such as the widely used 2-point statistics in configuration and Fourier spaces. In this work, for the first time, we present the differences in the morphology of the large scale structure caused by modifications to general relativity (to address the cosmic acceleration problem), by measuring the MFs from N-body simulations of modified gravity and general relativity. We find strong statistical power when using the MFs to constrain modified theories of gravity: with a galaxy survey that has survey volume $\sim 0.125(h^{-1}\ \mathrm{Gpc})^3$ and galaxy number density $\sim 1/(h^{-1}\ \mathrm{Mpc})^3$, the two normal-branch Dvali-Gabadadze-Porrati models and the F5 $f(R)$ model that we simulated can be discriminated from the ΛCDM model at a significance level $\gtrsim 5\sigma$ with an individual MF measurement. Therefore, the MF of the large scale structure is potentially a powerful probe of gravity, and its application to real data deserves active exploration.

Introduction.—Gravity is one of the most fundamental forces that shape our world, and its effect is felt from very small scales—in our everyday life—to very large scales—in the evolution of our Universe. The year of 2015 celebrated the centenary of our standard theory of gravity—Einstein's general relativity (GR)—which has withstood various rigorous tests. Less attention, however, has been paid to the unsettling fact that these tests were primarily carried out in small systems such as our Solar System, and the application to cosmology is an extrapolation dramatically outside the regime where the theory is confirmed experimentally. The discovery of the accelerating Hubble expansion in the late Universe [1,2], indeed, lends support to the suspicion that gravity may not be strictly Einsteinian on cosmic scales. Studies of cosmological tests of gravity, therefore, can address these two fundamental questions simultaneously.

There has been a growing body of recent research on testing gravity in cosmology. Most of these studies employ traditional measurements of the geometry and structure formation of the Universe, such as the type Ia supernovae, baryonic acoustic oscillations, gravitational lensing, galaxy clustering, and clusters of galaxies. These observables have their advantages and disadvantages, and are usually complementary to each other. The bottom line, however, is that the real Universe has a very complicated structure, which can rarely be fully described by a single observable. Therefore, it is critical that other statistical properties of the same observations, which encode additional information, are also exploited to improve the constraining power on theoretical models.

In this work, we propose a new probe of gravity using the morphology of the cosmic large-scale structure (LSS) as specified by its four Minkowski functionals (MFs). According to Hadwiger's theorem [3], for a spatial pattern in 3D, its morphological properties defined as satisfying motion invariance (i.e., invariant under rotation and translation), Minkowski additivity (i.e., the property of a union of domains is the sum of those of the individual domains minus that of the overlapping domain), etc., are completely specified by four MFs. In studying the MFs of the LSS, the patterns are most commonly taken to be the excursion sets of a smoothed density field (such as galaxy number density, matter density) [4–6], i.e., regions of space with field value above some specified threshold, which is what we adopt in this work, see Refs. [7,8] for other choices of patterns. Geometrically, up to a constant multiplicative factor, the four MFs from the zeroth to the third order represent, respectively, the pattern's volume, its surface's area, integrated mean curvature, and Euler characteristic (or genus [9,10]).

The MFs are complementary to other statistical observables in probing the LSS. While the N-point correlation functions in real space or the corresponding polyspectra in Fourier space probe the statistics of the LSS at specific orders, the MFs comprehensively probe all orders of statistics. Compared to the higher order ($n > 2$) statistics whose measurements are usually cumbersome to obtain, the MFs can be easily measured. Moreover, the MFs have

the advantage of being more robust to systematic effects such as nonlinear gravitational evolution and biases of the LSS tracers [6,10], compared to the N-point statistics. For example, on linear scales, the MFs measured with different tracers of the LSS are all the same, i.e., independent on tracer biases, which is an advantageous feature that N-point statistics measurements do not have.

The MFs were introduced into cosmology by Ref. [7] in 1994. Since then, most studies on its application have been focused on examining the (non-)Gaussianity of primordial perturbations, from observations of not only the LSS [11] but also the cosmic microwave background [12], though several other interesting applications have also been proposed [13]. In particular, its potential in probing gravity was only addressed for the 2D weak lensing convergence field in Ref. [14]. In this Letter, motivated by the strong statistical power from ongoing and future LSS surveys, we investigate the potential of these morphological descriptors of the LSS in discriminating different theories of gravity. We will base our results on N-body simulations with modified gravity and GR. We notice relevant previous theoretical work by Ref. [15] that used the scaling of the genus statistic of the LSS with smoothing scale as a probe of gravity, and relevant discussions by Codis *et al.* in Ref. [11].

Gravity models and simulations.—As an illustration, we consider two classes of modified gravity models: the Hu-Sawicki $f(R)$ gravity model [16] and the normal-branch Dvali-Gabadadze-Porrati (hereafter NDGP) model [17,18] (the self-accelerating branch is known to suffer from both observational and theoretical difficulties [19]). In each class, we study two models with different parameter values: for $f(R)$ gravity, these are obtained by setting the $f(R)$ parameter f_{R0} to -10^{-6} (F6) and -10^{-5} (F5) respectively, with larger values of $|f_{R0}|$ implying stronger deviations from standard gravity; we tune the NDGP parameter r_c so that the value of σ_8, the rms linear density perturbation in spherical regions of radius $8h^{-1}$ Mpc at $z = 0$, is equal to that in the models of F6 and F5 (specifically, $r_c = 5.7H_0^{-1}$ and $1.2H_0^{-1}$, respectively, with H_0 the Hubble parameter)—these are dubbed NDGP_F6 and NDGP_F5, respectively. Current constraints on f_{R0} and r_c using other cosmological probes are $|f_{R0}| \lesssim 10^{-5}$ [20] and $r_c \gtrsim H_0^{-1}$ [21] at the 95% C.L., and we expect the MFs of the LSS can further tighten these results. Finally, note these models are designed to have the same background expansion as the ΛCDM model.

Our analysis is based on simulations of the above models using the ECOSMOG code [22,23]. All simulations started at $z = 49$ with the same (best-fit WMAP 9 yr [24]) cosmological parameters and initial conditions. These are specifically designed to separate effects of the modified gravitational law from those of cosmic variance, background expansion history, and other variations in parameters. In all simulations, we evolve 1024^3 dark matter particles in a cubic box with length $1024h^{-1}$ Mpc a side, which is covered by a regular mesh with 1024^3 cells.

The cells are refined if they contain more than eight particles, and such an adaptive refinement scheme [25] ensures high force resolution in dense regions, where modified gravity effects are hard to calculate.

We point out that we have made the hypothesis, following the standard paradigm, that Newtonian simulations for first-order GR perturbations that average out on a Friedmann-Lemaître-Robertson-Walker background cosmology faithfully represent structure formation. We call this case "GR" to distinguish this scenario from corresponding realizations of modified gravity models, the quasistatic approximation used in which is well checked [26]. We emphasize, however, that the standard paradigm is not based on full GR simulations. It may well be that deviations in the form of cosmological backreaction to account for this difference [27] could display similar signatures as those of modified gravity models. Our work may imply that backreaction effects could also be quantified by measurement of the MFs.

Measurement of Minkowski functionals.—We measure the MFs for the excursion sets of dark matter density field. The procedures are as follows. We obtain dark matter density from positions of particles in our simulations using the cloud-in-cell technique. The density field is subsequently smoothed by a Gaussian window function with size R_G. The MFs are then measured for the smoothed field as a function of ρ, the density threshold used to define the excursion set. Based on either differential geometry or integral geometry, two standard methods to measure the MFs are developed in [4], i.e., the one using the Koenderink invariant and the one using the Crofton's formula. In our calculations, we find the two methods give consistent results. Therefore, we will simply quote our results using the method based on the Crofton's formula.

We denote the four MFs as V_i, with $i = 0, 1, 2, 3$ specifying their order. Therefore, V_0 is the volume fraction of the excursion set, while V_1, V_2, V_3 are its surface's area, integrated mean curvature, and Euler characteristic per unit volume respectively (see e.g., [4] for exact prefactors in the definitions). The geometrical meaning of V_3 may deserve more explanation: it is equal to the genus statistic ($g \equiv$ number of holes minus number of disjoint regions) [9,10] except for a minus sign; therefore, it describes the connectedness of the isodensity contours. $V_3 > 0$ means more disconnected contours, otherwise, more connected.

Results.—To highlight the differences in the MFs caused by modified gravity, we measure and compare the MFs for different models at $z = 0$, since the effects of modifications to gravity are generally larger at a lower redshift [22,23]. We choose the smoothing scale R_G to be $5h^{-1}$ Mpc, which is large enough to suppress the shot noise without smearing out the important differences in the MFs.

Our results are presented in Fig. 1. In the left panel, we show the MFs themselves, while the differences in the MFs between modified gravity models and ΛCDM, the ΔV_is, are displayed in the right panel. We show the results for
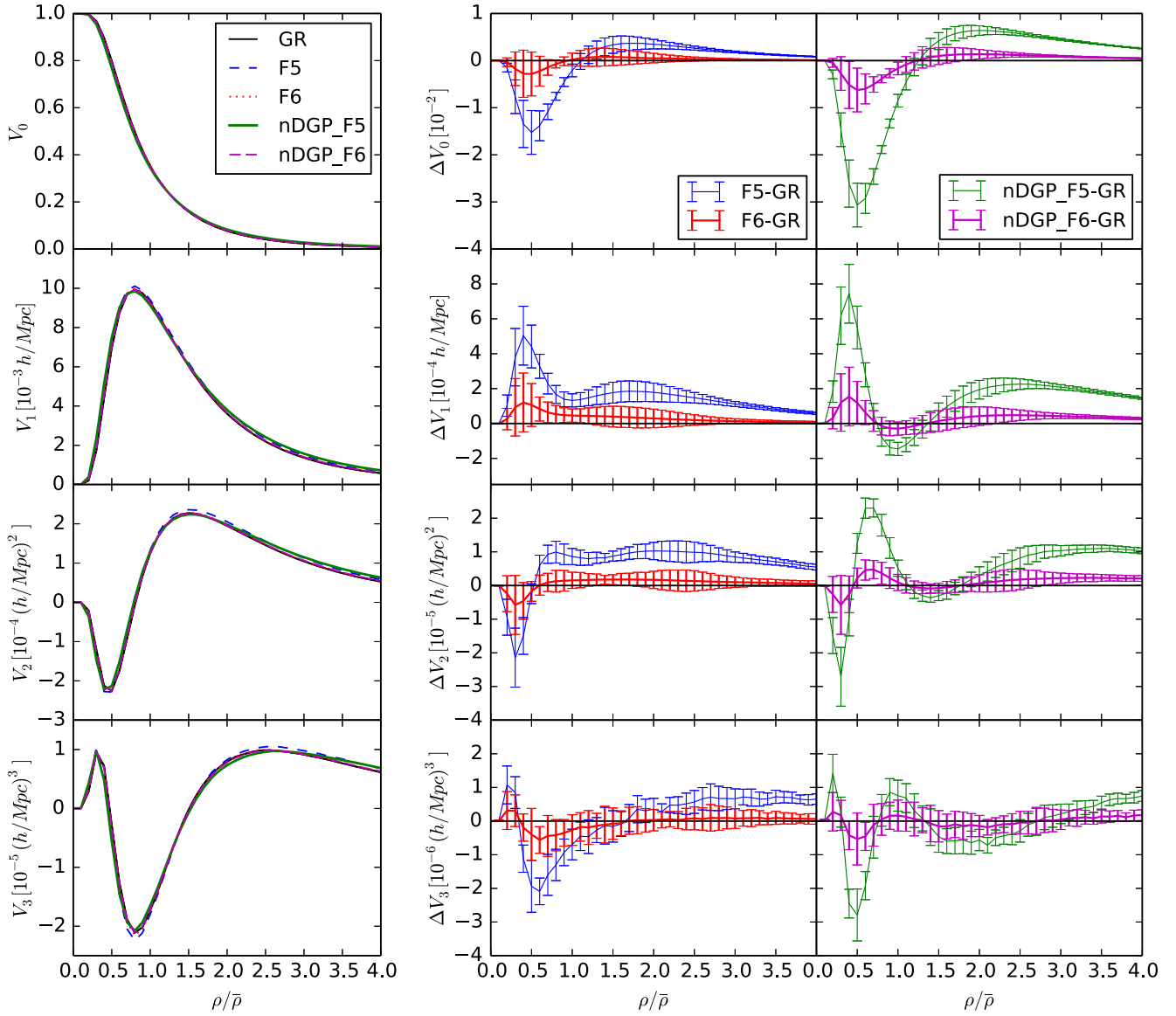
FIG. 1.   Left panel: The MFs of the LSS computed from *N*-body simulations for different models of gravity at $z = 0$ and with $R_G = 5h^{-1}$ Mpc. The two $f(R)$ models (F5, F6) and two NDGP models (NDGP_F5, NDGP_F6) have the same background expansion as the GR case, i.e., the ΛCDM model, see text for more details. Right panel: The differences in the MFs between modified gravity models and GR, first column for $f(R)$, and second column for NDGP. $\rho/\bar{\rho}$ is the density threshold used for the MF calculations in ratio of the mean density.

$\rho/\bar{\rho}$, the ratio of the density threshold to the mean density, in the range of [0, 4], over which we find the signal-to-noise (S/N) ratio for the MF is most significant. We estimate the error bars by subdividing our original simulation box into eight equal-sized sub-boxes, each with a volume $512^3 h^{-3}$ Mpc^3 (for small error bars and for convenience of the calculation), and taking the standard deviations of the MFs measured for each sub-box. These are displayed in the right panel of Fig. 1. We note here that the idealistic way to estimate the error bars is by running a large ensemble of simulations (a highly computationally expensive task which we postpone for future work), and subdividing the simulation box is only indicative for the idealistic error estimation. In the following, we focus on understanding the

ΔV_is. The curves of the MFs themselves share similar trends as a Gaussian random field, which have been well studied in the literature, see, e.g., Ref. [6]. Therefore, in the following, they are mentioned only for the purpose of helping us to understand the ΔV_is.

Overall, we find the differences in the MFs caused by the two $f(R)$ models have the same trend. However, as the modification to gravity is stronger in F5, ΔV_i in this model has a higher amplitude. The same results hold true for the two NDGP models. While compared with the $f(R)$ model, ΔV_i in the corresponding NDGP model that has the same σ_8 as $f(R)$ also has a higher amplitude and more features, though shares a similar trend. This is because the σ_8 values for $f(R)$ gravity and NDGP are calculated using linear

perturbation theory; in $f(R)$ gravity, this overestimates the modified gravity effect by neglecting the chameleon screening, so that the effect in a realistic universe, fully captured by the nonlinear simulations, is actually smaller than suggested by the value of σ_8; while for NDGP, the screening is weak on linear scales, so that the σ_8 value is a reasonably accurate description of the realistic case.

Specifically, for V_0, the volume fraction occupied by regions whose densities are above a given threshold, we find the modified gravity in both $f(R)$ and NDGP makes it larger when the threshold $\rho/\bar{\rho} \gtrsim 1$ and smaller when $\rho/\bar{\rho} \lesssim 1$. That is, the volume fraction with density above an overdensity threshold gets larger, while above an underdensity threshold gets smaller. The latter is equivalent to that the volume fraction with density below an underdensity threshold gets larger. These findings are consistent with the picture that both haloes and voids are more abundant and/or bigger in the two models [28]. One can also infer that this trend is stronger in NDGP than in the corresponding $f(R)$ model for the same reason as mentioned above, as one finds in Fig. 1.

For the excursion sets' surface area V_1, its difference caused by the two kinds of modification to gravity roughly follows that of their volume fraction V_0, except at the very low density threshold region ($\rho/\bar{\rho} \lesssim 1$ for $f(R)$ and $\lesssim 0.8$ for NDGP) where the changes are in opposite directions. This can be understood as follows: if the excursion sets are all isolated regions, as is the case for a high enough density threshold, it is reasonable to expect that the change in their surface area follows that in the volume fraction they occupy. However, for very low density threshold, though the isodensity contours are still isolated, their enclosed regions are no longer the excursion sets, but under-dense regions with density below the threshold, whose volume fraction is therefore $(1 - V_0)$. Thus, at the very low density threshold region, V_1 changes in the opposite direction as V_0, and becomes larger in both $f(R)$ and NDGP.

For V_2, the integration of the mean curvature of the excursion sets' surface over the surface area, we find it to be negative (positive) when $\rho/\bar{\rho} \lesssim 0.8 (\gtrsim 0.8)$ in all the models we study. This is understandable considering that the positive direction of the surface points toward lower density regions. Specifically, when the density threshold is high enough, the excursion sets will be isolated high density regions with closed surfaces whose positive directions point outward, and therefore, the mean curvature is positive; while when the density threshold is low enough, the excursion sets will be the complement of isolated low density regions with closed surfaces whose positive directions now point inward, and therefore, the mean curvature is negative. The transition from positive to negative of the integrated mean curvature happens at $\rho/\bar{\rho} \simeq 0.8$ in the models we study. Suppose the change in the mean curvature is negligible, one can expect that V_2 changes in the opposite (same) direction as V_1 when $\rho/\bar{\rho} \lesssim 0.8 (\gtrsim 0.8)$, since the surface area is always positive (note, V_2 is roughly

the mean curvature times the area). This is roughly the case for ΔV_2 when $\rho/\bar{\rho}$ is far enough from 0.8 in both the $f(R)$ and NDGP models. While, when $\rho/\bar{\rho}$ approaches 0.8 and where this phenomenon does not hold, the change in the mean curvature plays a more important role, and we find V_2 gets larger in both models. Combined with the specific changes in V_1, one can infer that the mean curvature gets larger for the isodensity contours specified with these density thresholds.

As for the connectedness evaluated by comparing the number of holes through the structure of the excursion sets and the number of disjoint parts in it, we find the isodensity contours are more connected with $V_3 < 0$ (i.e., more holes) when $0.5 \lesssim \rho/\bar{\rho} \lesssim 1.5$, but more isolated with $V_3 > 0$ (i.e., more disjoint parts) elsewhere. For $f(R)$, we find the modification to gravity makes this behavior more evident; i.e., V_3 is larger (smaller) where it is positive (negative). This is also roughly the case for NDGP, except that V_3 gets larger around $\rho/\bar{\rho} \simeq 0.8$ where it was most negative, that is, the contours are less connected where they were most connected. This difference highlights the different modifications to gravity in the two models, and together with other differences in the ΔV_is, can be used to discriminate one from the other.

With our estimation for the error bars, we find that the MFs can easily discriminate the modified gravity models of NDGP_F5, NDGP_F6, and F5 from GR: with an individual MF measurement, these models can be discriminated from GR with a significance level up to ~ 30, 10, and 5σ. Though for F6, individual MF measurement can only tell it from GR at the level of 1σ at most, combining the different orders of MFs at different thresholds can probably boost the level to be significant enough. We also note that the error bars we obtained from simulations are appropriate for a galaxy survey with survey volume of $0.125h^{-3}$ Gpc^3 (corresponding to observing the full sky from $z = 0$ to $z \simeq 0.1$) and with galaxy number density of $1h^3$ Mpc^{-3}, which are more optimistic compared to the galaxy surveys nowadays. However, considering the strong statistical power we have found and considering the gains from combining the MFs of different orders, at different thresholds, with different smoothing scales and at different redshifts, we expect the MFs can provide a powerful probe of gravity, especially for those ambitious galaxy surveys with large survey volumes and high galaxy densities such as DESI [29]. We leave such a comprehensive study with real surveys for future work [30].

Conclusions.—The morphological properties of the LSS described by the four MFs provide important complementary information to other statistics. In this Letter, we investigate their potential as a new probe of gravity. By using N-body simulations of modified gravity and GR, we disclose the morphological differences in the LSS caused by modified gravity, and provide insights to understand the differences in the MFs. With the estimated errors for a galaxy survey with volume of $0.125h^{-3}$ Gpc^3 and galaxy

number density of $1h^3$ Mpc^{-3}, we find the modified gravity models of NDGP_F5, NDGP_F6, and F5 can be discriminated from GR with a significance level up to ∼30, 10, and 5σ with just an individual MF measurement. This strong statistical power of the MFs as a probe of gravity can probably survive in ambitious real galaxy surveys with smaller survey areas and lower galaxy densities, providing the MFs of different orders, at different thresholds, with different smoothing scales and at different redshifts are combined together. We pursue such a comprehensive study in an ongoing work [30].

---

*Corresponding author.
wjfang@ustc.edu.cn
†baojiu.li@durham.ac.uk
‡gbzhao@nao.cas.cn

[1] S. Perlmutter *et al.* (Supernova Cosmology Project), Astrophys. J. **517**, 565 (1999).

[2] A. G. Riess *et al.* (Supernova Search Team), Astron. J. **116**, 1009 (1998).

[3] H. Hadwiger, *Vorlesungen über Inhalt, Oberfläche und Isoperimetrie* (Springer, Berlin, 1957).

[4] J. Schmalzing and T. Buchert, Astrophys. J. **482**, L1 (1997).

[5] C. Hikage, J. Schmalzing, T. Buchert, Y. Suto, I. Kayo, A. Taruya, M. S. Vogeley, F. Hoyle, J. R. Gott, III, and J. Brinkmann, Publ. Astron. Soc. Jpn. **55**, 911 (2003).

[6] C. Blake, J. B. James, and G. B. Poole, Mon. Not. R. Astron. Soc. **437**, 2488 (2014).

[7] K. R. Mecke, T. Buchert, and H. Wagner, Astron. Astrophys. **288**, 697 (1994).

[8] A. Wiegand, T. Buchert, and M. Ostermann, Mon. Not. R. Astron. Soc. **443**, 241 (2014).

[9] J. R. Gott, III, M. Dickinson, and A. L. Melott, Astrophys. J. **306**, 341 (1986).

[10] T. Matsubara, Astrophys. J. **584**, 1 (2003).

[11] See, e.g., Ref. [5] and C. Hikage, E. Komatsu, and T. Matsubara, Astrophys. J. **653**, 11 (2006); S. Codis, C. Pichon, D. Pogosyan, F. Bernardeau, and T. Matsubara, Mon. Not. R. Astron. Soc. **435**, 531 (2013).

[12] See, e.g., J. Schmalzing, and K. M. Gorski, Mon. Not. R. Astron. Soc. **297**, 355 (1998); C. Hikage, T. Matsubara, P. Coles, M. Liguori, F. K. Hansen, and S. Matarrese, Mon. Not. R. Astron. Soc. **389**, 1439 (2008); W. Fang, A. Becker, D. Huterer, and E. A. Lim, Phys. Rev. D **88**, 041302 (2013); P. A. R. Ade *et al.* (Planck Collaboration), Astron. Astrophys. **594**, A17 (2016); T. Buchert, M. J. France, and F. Steiner, arXiv:1701.03347.

[13] See, e.g., J. Sato, M. Takada, Y. P. Jing, and T. Futamase, Astrophys. J. **551**, L5 (2001); C. Park, J. Kim, and J. R. Gott, III, Astrophys. J. **633**, 1 (2005); L. Gleser, A. Nusser, B. Ciardi, and V. Desjacques, Mon. Not. R. Astron. Soc. **370**, 1329 (2006); C. Park and Y.-R. Kim, Astrophys. J. **715**, L185 (2010); J. M. Kratochvil, E. A. Lim, S. Wang, Z. Haiman, M. May, and K. Huffenberger, Phys. Rev. D **85**, 103513 (2012); C. Beisbart, R. Valdarnini, and T. Buchert, Astron. Astrophys. **379**, 412 (2001).

[14] C. Ling, Q. Wang, R. Li, B. Li, J. Wang, and L. Gao, Phys. Rev. D **92**, 064024 (2015); D. Munshi, B. Hu, T. Matsubara, P. Coles, and A. Heavens, J. Cosmol. Astropart. Phys. 04 (2016) 056; M. Shirasaki, T. Nishimichi, B. Li, and Y. Higuchi, Mon. Not. R. Astron. Soc. **466**, 2402 (2017).

[15] X. Wang, X. Chen, and C. Park, Astrophys. J. **747**, 48 (2012).

[16] W. Hu and I. Sawicki, Phys. Rev. D **76**, 064004 (2007).

[17] G. R. Dvali, G. Gabadadze, and M. Porrati, Phys. Lett. B **485**, 208 (2000).

[18] F. Schmidt, Phys. Rev. D **80**, 123003 (2009).

[19] W. Fang, S. Wang, W. Hu, Z. Haiman, L. Hui, and M. May, Phys. Rev. D **78**, 103509 (2008); M. A. Luty, M. Porrati, and R. Rattazzi, J. High Energy Phys. 09 (2003) 029; A. Nicolis and R. Rattazzi, J. High Energy Phys. 06 (2004) 059; K. Koyama, Classical Quantum Gravity **24**, R231 (2007).

[20] M. Cataneo, D. Rapetti, F. Schmidt, A. B. Mantz, S. W. Allen, D. E. Applegate, P. L. Kelly, A. von der Linden, and R. G. Morris, Phys. Rev. D **92**, 044009 (2015); X. Liu *et al.*, Phys. Rev. Lett. **117**, 051101 (2016); S. Peirone, M. Raveri, M. Viel, S. Borgani, and S. Ansoldi, Phys. Rev. D **95**, 023521 (2017).

[21] A. Barreira, A. G. Sanchez, and F. Schmidt, Phys. Rev. D **94**, 084022 (2016).

[22] B. Li, G.-B. Zhao, R. Teyssier, and K. Koyama, J. Cosmol. Astropart. Phys. 01 (2012) 051.

[23] B. Li, G.-B. Zhao, and K. Koyama, J. Cosmol. Astropart. Phys. 05 (2013) 023.

[24] G. Hinshaw *et al.*, Astrophys. J. Suppl. Ser. **208**, 19 (2013).

[25] R. Teyssier, Astron. Astrophys. **385**, 337 (2002).

[26] S. Bose, W. A. Hellwing, and B. Li, J. Cosmol. Astropart. Phys. 02 (2015) 034.

[27] T. Buchert and S. Räsänen, Annu. Rev. Nucl. Part. Sci. **62**, 57 (2012).

[28] B. Li, G.-B. Zhao, and K. Koyama, Mon. Not. R. Astron. Soc. **421**, 3481 (2012).

[29] http://desi.lbl.gov.

[30] W. Fang, B. Li, G.-B. Zhao, C. Howlett, and W. Percival (to be published).